

## Assembly strategies of wind turbine towers for minimum fatigue damage

Cristina Nunez-Casado<sup>1</sup>, Oscar Lopez-Garcia<sup>\*1</sup>, Enrique Gomez de las Heras<sup>2</sup>, Alvaro Cuerva-Tejero<sup>1</sup> and Cristobal Gallego-Castillo<sup>1</sup>

<sup>1</sup>Departamento de Aeronaves y Vehiculos Espaciales, ETSIAE, Universidad Politecnica de Madrid, Spain

<sup>2</sup>Siemens Gamesa Renewable Energy

(Received March 28, 2017, Revised November 10, 2017, Accepted November 13, 2017)

**Abstract.** The aim of this paper is to present a method to obtain the dynamic response of a wind turbine tower in time domain by means of the generation of time series and to estimate the associated fatigue damage by means of a Rainflow counting algorithm. The proposed method is based on assuming the vortex shedding is a bidimensional phenomena and on following a classical modal superposition method to obtain the structure dynamic response. Four different wind turbine tower geometric configurations have been analyzed in a range of usual wind velocities and covering extreme wind velocities. The obtained results have shown that, depending on the turbulence intensity and the mean wind velocity, there are tower geometric configurations more advantageous from the fatigue load standpoint. Consequently, the presented model can be utilized to define assembly strategies oriented to fatigue damage minimization.

**Keywords:** vortex shedding; fatigue damage; wind turbine towers; assembly process; rainflow

### 1. Introduction

Dynamic response induced by vortex shedding appears in many engineering fields, among them, in the wind energy field. Modern large wind turbines are formed by slender structures such as the tower that are highly sensitive to loads induced by vortex shedding, being a concerning situation for wind turbine manufacturers who design different tools to prevent the vortex shedding effect such as the one reported in Llorente Gonzalez (2006). Vortex shedding induced loads are an important source of fatigue damage for wind turbine towers. Fatigue damage assessment and detection of wind turbine towers is an important and active research topic as the recent literature suggests. For instance, Berny-Brandt and Ruiz (2016) presents a probabilistic approach that combines structural demand hazard analysis with cumulative damage assessment applied to a steel tower of a wind turbine. Vibration-based damage detection studies have been recently proposed in the literature. Nguyen *et al.* (2017)

---

\*Corresponding author, E-mail: [oscar.lopez.garcia@upm.es](mailto:oscar.lopez.garcia@upm.es)

develop a hybrid damage detection method for wind turbine tower structures by measuring vibration and impedance responses. Nguyen *et al.* (2015) propose two vibration-based damage detection methods for wind turbine towers. The first one is a frequency-based damage detection method and the second one is a mode-shape-based damage detection model. Erection of wind turbines can take several weeks or months. During this time, wind conditions can cause large amplitude varying displacements of wind turbine towers that can even consume an important part of the towers fatigue life. Although Trivellato and Castelli (2015) collect models to compute the Strouhal number and apply them to several wind turbine configurations in operating conditions, as far as the authors' knowledge is concerned, the fatigue damage due to vortex shedding of wind turbine towers during the assembly process has not been analyzed before. However, there are other slender structures, similar to wind turbine towers, subjected to vortex shedding loads, whose fatigue damage has been reported, see Repetto and Solari (2010), which justifies the importance of this paper. Assessment of the dynamic response can be very useful, in such a way that the assembly process can be managed by choosing the appropriate geometric configurations for the tower, composed of different sections, that are more advantageous in terms of fatigue damage.

As stated in Dyrbye and Hansen (1997), there are two main methods to estimate vortex shedding structural response, the spectral method and the vortex resonance model. Spectral vortex shedding methods are based on the contributions of Vickery and Clark (1972), where the mathematical model is presented, and developed thoroughly in Vickery and Basu (1983b) and Vickery and Basu (1983a). This model is able to reproduce the main vortex shedding features such as the lock-in phenomenon, in which the vortex shedding frequency equals the vibration frequency. From engineering point of view the Canadian Code, the CICIND model and the second approach of Eurocode-1 (2010) are the most used spectral methods. On the other hand, authors like Hansen (1998) and Verboom and Van Koten (2010) propose approaches based on the model of Vickery and Basu (1983b) which improve, among other things, the aerodynamic damping modeling by means of considering the turbulence intensity influence. These modifications lead to obtain a better cross-wind dynamic response prediction in contrast to the overestimation obtained by the second approach of Eurocode-1 (2010), see the comparison performed by Verboom and Van Koten (2010) for 13 industrial chimneys. Among the models derived from Vickery and Basu (1983b), it should be also stressed the model proposed by Gorski (2009) which solves numerically the structural dynamic response including the lateral turbulence loads. Related to the Vickery and Basu (1983b) model there are methods such as the model presented in Chen (2013), proposed for slender buildings, which uses the high-frequency-force-balance technique to quantify the vortex shedding load, without knowing its time-space description, from the base bending moment measurements in a wind tunnel. On the other hand, Eurocode-1 (2010) proposes a non spectral vortex shedding method which is the vortex resonance model, see Ruscheweyh (1994). In spite of this great amount of research work to predict the crosswind response of slender structures, semi-empirical models are still far away from being able to model all the involved processes in the vortex shedding phenomenon. For this reason, some recent researches, such as the couple structure-fluid model proposed by Belver *et al.* (2012), are focused on studying the vortex-induced structural response by means of computational fluid dynamics (CFD).

The spectral vortex shedding model proposed by Vickery and Basu (1983b) describes the vortex shedding loads through two contributions, a stochastic load defined by a stationary stochastic process and a motion induced force function of the structure response. Depending on the structural properties and operational conditions, one of the two loads is predominant, which takes the structure to present a low stochastic response or a large self-excited harmonic response, respectively. The model presented in this study is based on the loads description carried out by Vickery and Basu (1983b) obtaining the structure dynamic response through the time domain approach. This approach enables to apply a nonlinear description of the motion induced force without any additional simplification derived from the use of the frequency domain linear formulation.

In this paper a time domain approach is presented to evaluate fatigue damage using the Rainflow Counting method (RFC), see E1049-85 (1985) and applied to a real wind turbine tower. The advantages of such an approach are computation of displacement and bending moment distributions, determination by numerical simulations of maximum values of displacements and bending moments, and direct assessment of fatigue damage. In Repetto and Solari (2002) and Chen (2014), other methods to estimate the structure fatigue damage due to vortex shedding are presented.

The remainder of the article is organized as follows: Section 2 describes the fluid-structure model. Appropriate parameter values of the proposed algorithm and the aerodynamic damping model are discussed in Section 3. The main results are presented in Section 4. Section 5 connects the obtained results with the definition of optimal assembly strategies from the fatigue damage minimization standpoint. The paper ends with the main conclusions and future lines of research gathered in Section 6.

## 2. Model description

The time domain approach followed here is supported by the studies addressed by Vickery and Clark (1972) and Vickery and Basu (1983b), which are based on obtaining a time-space description of the vortex shedding load and on incorporating a nonlinear aerodynamic damping to model the motion induced forces. The description of the model has been carried out as follows: Section 2.1 describes the structural model while Section 2.2 analyzes in depth the vortex shedding load defined in Vickery and Basu (1983b). Section 2.3 develops the time domain approach and, finally, the assessment of fatigue is addressed in Section 2.1.

### 2.1 Structural model

The wind turbine tower is modeled as one-dimensional beam defined by its distribution of mass and bending stiffness. As a first estimation, the nacelle and stopped rotor are considered as point masses located at the tower tip. In the most general case, the tower is composed of five section, nacelle and stopped rotor, therefore, the structural model is developed for this tower geometric configuration. The particular case of considering a tower composed of four or five sections is recovered after cancelling the terms depending on the point mass. Fig. 1 shows the reference frame and structural models of the four tower geometric configurations considered in Section 3 and 4. It should be stressed that TG125-R

and TG125-G towers differ in the mass point value. Applying the Principle of least action, considering the kinetic energy, the elastic potential energy and the gravitational potential energy, the partial differential equation which defines the structural model is obtained as

$$m(z)\ddot{q} + \frac{\partial^2}{\partial z^2} \left( EI(z) \frac{\partial^2 q}{\partial z^2} \right) = f_v + f_m, \quad (1)$$

where  $q$  is the displacement,  $f_v$  the stationary vortex shedding load and  $f_m$  the motion induced load. It can be observed that the point mass dependency comes from the boundary conditions, also obtained from the Principle of least action,

$$q \Big|_0 = 0, \quad \left( \frac{\partial q}{\partial z} \right) \Big|_0 = 0, \quad EI \frac{\partial^2 q}{\partial z^2} \Big|_H = 0, \quad \left( \frac{\partial}{\partial z} EI \frac{\partial^2 q}{\partial z^2} \right) \Big|_H - M \ddot{q} \Big|_H = 0. \quad (2)$$

Considering the tower tip point mass modifies the boundary conditions compared to the four-section and five-section tower, in such a way that, now, the force in section  $z = H$  is not zero and a balance of forces has to occur between the elastic force and the inertial force due to the point mass, see the fourth equation in Eq. (2).

Cancelling the external forces of Eq. (1), and using the separation of variables method, the eigenvalues and eigenvectors problem is obtained which allows to compute the eigenfrequencies and eigenmodes. Appendix A shows the modal analysis of the tower configurations analyzed in Section 3 and 4.

## 2.2 Vortex induced load model

Vickery and Basu (1983b) define the crosswind load by means of two forces acting on the structure: the vortex shedding load itself and the motion induced load. The vortex

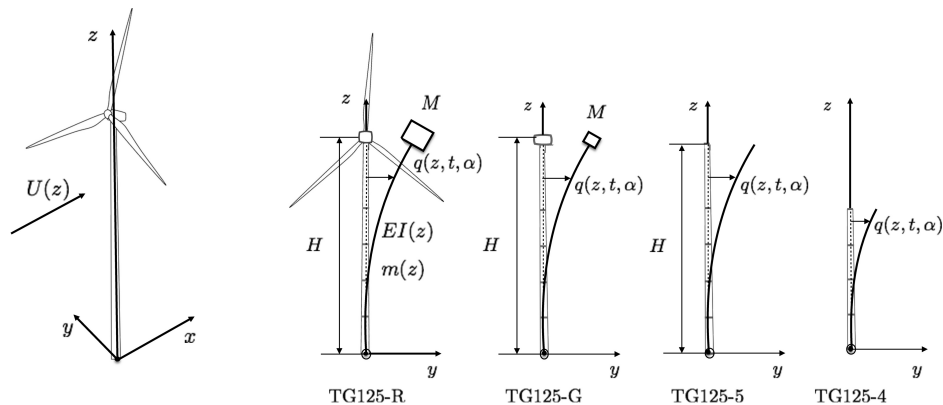


Fig. 1 Reference frame and definition of the wind turbine tower configurations. Left hand figure shows the real wind turbine while, on the right hand figures, the structural models are shown for the four tower geometric configurations considered in Section 4, where  $m(z)$  is the mass per unit of length,  $EI(z)$  the bending stiffness,  $M$  the point mass and  $q(z, t, \alpha)$  is the tower displacement which depends on height, time and stochastic realization

shedding load,  $f_v$ , exists whether or not the structure is moving. The turbulent nature of the atmospheric flow makes the vortex shedding load exhibit a stochastic behavior. Vickery and Basu (1983b), through pressure measurements on a rigid tower and subsequent integration on the surface tower, obtain a time-space description of the crosswind load and describe the vortex shedding load as a stationary stochastic process defined by the power spectral density (PSD) of the lift coefficient,  $S_{c_l}$ , expressed in nondimensional form as

$$\frac{f S_{c_l}(z, f)}{\sigma_{c_l}^2} = \frac{f}{\sqrt{\pi} f_{vs}} \exp \left[ - \left( \frac{1 - \frac{f}{f_{vs}}}{B(z)} \right)^2 \right], \quad (3)$$

where  $f_{vs} = \text{St} U(z)/D(z)$  is the vortex shedding frequency related to the Strouhal number,  $\text{St}$ , the mean velocity,  $U$ , and the tower diameter,  $D$ . As regards the Strouhal number, it depends on the cross-section geometry, see Eurocode-1 (2010) for other cross-section geometries, and in this paper, is a constant value with the tower height. On the other hand,  $\sigma_{c_l}$  is the lift coefficient standard deviation dependent on the longitudinal wind turbulence intensity,  $I_u$ , and the integral length of turbulence,  $L(z)$ , and  $B(z)$  is the bandwidth parameter which is exclusively dependent on the longitudinal wind turbulence intensity,  $I_u$ , see Vickery and Basu (1983b). The wind turbulence intensity has been determined from the definition of the reference turbulence intensity,  $I_{\text{ref}}$  in accordance with IEC-61400-1 (2003).

The motion induced load arises when flexible structures are subjected to vortex shedding. In these structures, the vortex shedding load causes a dynamic response which, at the same time, is inducing an additional crosswind load. This additional load is referred to as motion induced force,  $f_m$ , and is characterized by being a nonlinear function of the structure velocity. It is necessary to stress that, for highly damped structures subjected to any wind velocity condition or for less damped structures when the wind velocity condition is below the lock-in region, a linear function with the structural response velocity is enough to model the motion induced force, see Vickery and Basu (1983b). Highly damped structures are those structures with larger structural damping than the aerodynamic damping associated with the vortex shedding phenomenon. The phenomenological model followed here is based on obtaining a motion induced force description from forced-vibration tests of structures in wind tunnel. In these tests, structures are subjected to harmonic excitations and the aerodynamic forces are measured. From the acquired information, the motion induced force description is generalized to any dynamic response, including for a random response. The actual vortex shedding forces based on the lift coefficient stochastic process is presented in the next subsection.

As regards the aerodynamic loads on the nacelle and rotor, the aerodynamic effect of these two elements has been neglected, as a first estimate, due to the lack of published data. However, the inertial influence of nacelle and stopped rotor has been handled in Section 2.1.

### 2.3 Time domain approach

The time domain approach requires the synthesis of force time series from the PSD. In order to generate the lift coefficient time series, the method provided in Veers (1988) has been used, which is originally developed for the generation of wind velocity time series. As stated

by Vickery and Basu (1983b), the vortex shedding stochastic process is narrow-banded, therefore, the Veers (1988) method has been combined with the harmonic superposition method, see Shinozuka and Deodatis (1991), in order to obtain the lift coefficient time series. Once the ensemble of the lift coefficient time series have been obtained, the crosswind load is obtained as the next stochastic process

$$f_v(z, t, \alpha_r) = \frac{1}{2} \rho U^2(z) D(z) c_l(z, t, \alpha_r), \quad (4)$$

where  $\rho$  is the air density,  $c_l(z, t, \alpha_r)$  the lift coefficient time series generated using the method described above, and  $\alpha_r$  denotes the stochastic realization number.

In what follows, the equations defining the fluid-structure model are obtained, avoiding an excessive mathematical development. From the structural model, Eq. (1), using the modal analysis method and considering uncoupled modal equations, the set of stochastic nonlinear ordinary differential equations which define the modal displacements,  $p_j$ , are obtained,

$$m_j \ddot{p}_j(t, \alpha_r) + 2m_j \omega_j (\zeta_s)_j \dot{p}_j(t, \alpha_r) + m_j \omega_j^2 p_j(t, \alpha_r) = f_j(t, \alpha_r) \quad j = 1, \dots, n_m, \quad (5)$$

where  $m_j$ ,  $\omega_j$ ,  $\zeta_s$ ,  $f_j$  and  $n_m$  are the modal masses, natural angular frequencies, structural modal damping ratios, modal forces and the considered number of structural modes, respectively. Observe that both, modal coordinates and modal forces are stochastic processes. The modal forces are composed of two terms, the modal vortex shedding forces and the modal motion induced forces,  $f_j = f_{v,j} + f_{m,j}$ . The modal vortex shedding forces are obtained projecting the vortex shedding force with each structural mode,

$$f_{v,j}(t, \alpha_r) = \frac{1}{2} \int_0^H \Psi_j(z) \rho U^2(z) D(z) c_l(z, t, \alpha_r) dz \quad (6)$$

with  $\Psi_j$  being the  $j$ -th structural mode. As stated by Vickery and Basu (1983b), the modal motion induced forces are composed of two terms, a linear term and nonlinear term of the modal velocity,

$$f_{m,j} = c_{a,j} \dot{p}_j - r_j \dot{p}_j^3 \quad j = 1, \dots, n_m \quad (7)$$

where the linear coefficient is defined as

$$c_{a,j} = 4\pi \rho f_{s,j} \int_0^H K_a(z) D(z)^2 \Psi_j^2(z) dz \quad j = 1, \dots, n_m, \quad (8)$$

and the nonlinear coefficient as

$$r_j = 4\pi \rho f_{s,j} G_j \int_0^H K_a(z) D(z)^2 \Psi_j^4(z) dz \quad j = 1, \dots, n_m \quad (9)$$

in which  $K_a(z)$  is the nondimensional aerodynamic damping parameter and  $G_j$  the limiting factor of dynamic response. According to Vickery and Basu (1983b), this last factor can be related to the maximum displacement,  $q_L$ , as

$$G_j = \left( \frac{1}{q_L \pi f_{s,j} \sqrt{3}} \right)^2. \quad (10)$$

The maximum displacement which has been fixed to  $0.4 D(H)$ , in accordance with Eurocode-1 (2010), being  $H$  the height of the tower. As mentioned above, in some cases the linear term is enough to model this force being dynamic response not very intense. However, in general, the nonlinear term is necessary to limit the tower maximum displacement at the tower tip to physical values, about one diameter. On the other hand, Vickery and Basu (1983b) has shown experimentally that the aerodynamic damping parameter depends on the Reynolds number,  $Re(z) = U(z)D(z)/\nu$ ; the reduced velocity,  $U_r(z) = U(z)/(f_{s,j}D(z))$  being  $f_{s,j}$  the structural resonance frequencies; and the longitudinal turbulence intensity,  $I_u(z)$ . Three aerodynamic damping models are described in Section 3.2, taking into account the latter dependencies. Once the aerodynamic damping parameter  $K_a(z)$  is defined, the modal aerodynamic damping is determined

$$\zeta_{a,j} = -\frac{\rho \int_0^H K_a(z)D(z)^2 dz}{m_j}. \tag{11}$$

By means of solving numerically each nonlinear ordinary differential equation using a time domain scheme, the modal displacements are obtained. Considering the modal decomposition, the tower displacement field is determined as

$$q(z, t, \alpha_r) = \sum_{j=1}^{n_m} \Psi_j(z) p_j(t, \alpha_r). \tag{12}$$

#### 2.4 Fatigue damage assessment

Fatigue damage is assessed from the base tower bending moment time series,  $M_{lt}(0, t, \alpha_r)$ , which are obtained from integrating the bending moment differential caused by the distributed structural loads along the tower height, second term of Eq. (1), and from adding the bending moment contribution due to the point mass acceleration,

$$M_{lt}(0, t, \alpha_r) = \int_0^H \frac{\partial^2}{\partial z^2} \left( EI(z) \frac{\partial^2 q}{\partial z^2} \right) z dz - M \ddot{q}(H, t, \alpha_r) H. \tag{13}$$

From the modal decomposition, see Eq. (12), and from the relation between the structural modes and the structural frequencies which comes from the separation of variables technique,

$$\frac{d^2}{dz^2} \left( EI(z) \frac{d^2 \Psi_j(z)}{dz^2} \right) = m(z) \Psi_j(z) \omega_j^2, \tag{14}$$

the tower base bending moment distribution along the tower height can be expressed as

$$M_{lt}(0, t, \alpha_r) = \sum_{j=1}^n \int_0^H m(z) \omega_j^2 \Psi_j p_j z dz - M \sum_{j=1}^n \ddot{p}_j (H - z). \tag{15}$$

In order to estimate fatigue damage, on the one hand, the RFC algorithm has been employed, see ASTM (1985). This method gives the number of cycles,  $n_i$ , and their amplitudes,

$S_i$ , of the time series corresponding to the tower base bending moment obtained from Eq. (15). On the other hand, it has been considered Miner's rule to accumulate fatigue damage in a linear form in accordance with IEC-61400-1 (2003). Specifically, in order to assess fatigue damage, the algorithm proposed by Nieslony (2009) is used. Following Ragan and Manuel (2007), the fatigue damage has been quantified through the damage equivalent load for a  $N$ -cycle time series,  $DEL_N$ , defined by

$$DEL_N(\alpha) = \left( \frac{1}{N} \sum_{i=1}^f n_i S_i^{m_f} \right)^{1/m_f}, \quad (16)$$

where  $m_f$  is the slope of the S-N fatigue curve. The damage equivalent load represents the load amplitude which produces, in a  $N$ -cycle time series, the same fatigue damage as the original time series.

### 3. Definition of parameters

Although Section 4 analyzes the four tower geometric configurations presented in Fig. 1, this section focuses on the five-section tower with nacelle and stopped rotor, referred to as TG125-R. Appendix A contains the necessary modal information related to this tower geometric configuration. Section 3.1 deals with the sensitivity to the time domain parameters, specifically, simulation time,  $t_{sim}$ , and number of stochastic realizations averaged,  $N_\alpha$ . On the other hand, Section 3.2 introduces and compares the aerodynamic damping models.

In both sections the tower tip displacement standard deviation is analyzed. Although this paper is focused on the fatigue assessment through the definition of the damage equivalent load, the displacement standard deviation, as well as, the bending moment standard deviation show the same tendency and all of them are equivalent in terms of the conclusions drawn for the displacement of the tower tip. The standard deviation is computed by first performing the standard deviation for fixed time of  $N_\alpha$  realizations and, next, carrying out a time average of the resulting time series.

Finally, it should be noted that the mean velocity and the longitudinal wind turbulence intensity have been defined according to the Normal Turbulence Model, NWP, and the Normal Turbulence Model, NTM, which are specified in IEC-61400-1 (2003). As regards the NWP, the reference height has been set to 125 m along all the paper while the reference velocity,  $U_{ref}$ , and the wind shear exponent,  $\alpha$ , are defined in the following sections.

#### 3.1 Algorithm parameters

The parameters which define the problem are of two types, physical such as the reference turbulence intensity or the reference velocity which have been described above, or related to the algorithm that are introduced in what follows. Among the latter, simulation time,  $t_{sim}$ , and number of stochastic realizations,  $N_\alpha$ , are the most relevant parameters. On the one hand, the number of realizations has to be enough to obtain a statistically independent result, and, on the other hand, the simulation time,  $t_{sim}$ , defines the frequency discretization in which the lift coefficient PSD is evaluated. Due to the fact that the lift coefficient PSD

is narrow-banded, the frequency discretization has to be small enough in order to the time series acquire all the features of the narrow band process.

Fig. 2(a) shows the displacement standard deviation at the TG125-R tower tip as a function of the reference velocity and for several number of realizations averaged. The nondimensional aerodynamic damping of these simulations corresponds to the one defined by Hansen (1998), see next Section 3.2 for a detailed discussion on aerodynamic damping modeling. The reference velocity range goes from 1 m/s up to 10 m/s. In these results, the simulation time has been fixed to 3600 s. The results show that using less than 24 realizations causes the curves to present abrupt peaks showing the statistical dependency with the ensemble of realizations generated from the stochastic process. If the number of stochastic realizations is fixed to  $N_\alpha = 48$ , the presented results are almost identical to the  $N_\alpha = 24$  case, but increasing the computation time because of the resolution of more time series. Fig. 2(b) presents the tower tip standard deviation as a function of the reference velocity for several values of the simulation time. The number of realizations has been fixed to 24, in such a way that the results are independent enough of the stochastic nature. The results show that, apart from a large number of averaged realizations, it is necessary to utilize time series at least of 3600 s in order to guarantee an appropriate time series generation. Considering the previous analysis, in what follows, the simulation time has been fixed to 3600 s and the number of realizations to 24.

### 3.2 Aerodynamic damping model

The mean velocity and the turbulence intensity have a great influence over the motion induced loads. Their effects are introduced in the model by means of the aerodynamic damping.

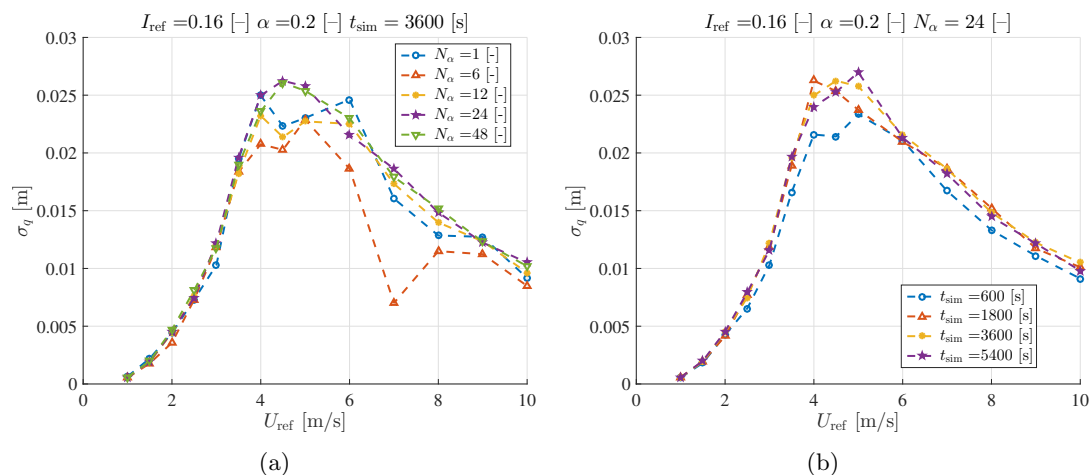


Fig. 2 Tower tip displacement standard deviation versus reference velocity,  $U_{\text{ref}}$ . Fig. (a) shows a stochastic realization average from 1 to 48, where the simulation time has been set to 3600 s. Fig. (b) analyzes the simulation time from 600 s to 5400 s, fixing the ensemble average to 24. Both analysis are performed on the TG125-R tower for a reference turbulence intensity of 0.16 and a wind shear exponent of 0.2

The aerodynamic damping parameter can be considered as a function of Reynolds number,  $Re$ , reduced velocity,  $U_r$  and reference turbulence intensity,  $I_{ref}$ , see Hansen (1998). In the case of vortex shedding in heavy towers with a high damping ratio, such as concrete towers, considering only the Reynolds dependency is enough to obtain results in agreement with experimental data, Vickery and Basu (1984). The reason is that, in these cases, the aerodynamic damping is much smaller than the structural one, and therefore, its variations are hardly noted in the total damping. As stated by Hansen (1998), keeping only the Reynolds number dependency in lighter and less damped structures, such as steel towers, where the aerodynamic damping is of the order of the structural one, causes models to obtain an extreme structural response. Due to technical reports, such as Tranvik and Alpsten (2002), it is known that such extreme structural response is associated with low turbulence intensities and mean velocities close to lock-in velocity where the magnitude of the dynamic response is increased in terms of tower tip displacement. In order to estimate the structural dynamic response in accordance with experimental results in the presence of any external condition, the turbulence intensity and reduced velocity dependencies have to be considered. Although the previous dependencies, Reynolds number, wind turbulence intensity and reduced velocity, have been described and verified in experimental results in Vickery and Basu (1983b), this reference together with the Eurocode-1 (2010), which is based on Vickery and Basu (1983b), only provide an aerodynamic damping model dependent on the Reynolds number. Hansen (1998) defines the aerodynamic damping parameter as a product of three factors, each of them depends on  $K_a(z) = K_{a_{max}}(Re) K_{I_u}(I_u) K_{U_r}(U_r)$  and is defined by the author as

$$K_{a_{max}}(z) = \begin{cases} 2, & Re(z) \leq 10^5 \\ 0.5, & Re(z) = 5 \times 10^5 \\ 1, & 10^6 \leq Re(z) \end{cases}, \quad (17)$$

$$K_{I_u}(z) = \begin{cases} 1 - 3 I_u(z), & 0 \leq I_u(z) \leq 0.25 \\ 0.25, & I_u(z) > 0.25 \end{cases}, \quad (18)$$

$$K_{U_r}(z) = \begin{cases} 0, & U_r St < 1 \\ -U_r St + 2, & 1 \leq U_r St \leq 2 \\ 0, & 2 < U_r St \end{cases}. \quad (19)$$

As regards the nondimensional aerodynamic damping term depending on the Reynolds number, a linear variation with the logarithm of the Reynolds number is assumed for  $10^5 < Re < 5 \times 10^5$  and for  $5 \times 10^5 < Re < 10^6$ . It should be noted that if the dependencies with the turbulence intensity and the reduced velocity are neglected in this latter model the description presented for the aerodynamic damping in Eurocode-1 (2010) is recovered.

In order to analyze the importance of the selected aerodynamic damping model, three different aerodynamic damping models are compared in this section. The first model is the one stated in Eurocode-1 (2010) which, as mentioned above, only depends on the Reynolds number. The third one corresponds to the three dependencies model of Hansen (1998) and the second one is a mixed model between the complete Hansen (1998) model and the Eurocode-1 (2010) model, in which the Reynolds number dependency and wind turbulence

intensity dependency are considered,  $K_a(z) = K_{a_{\max}}(\text{Re}) K_{I_u}(I_u)$ . This latter model is also introduced by Hansen (1998) and its function is to include the wind turbulence effect on the aerodynamic damping parameter which is estimated in smooth flow.

Fig. 3(a) shows the tower tip displacement standard deviation, for a wind turbulence intensity of 0.16, as a function of the reference velocity. Three curves for each model of aerodynamic damping are presented. Eurocode-1 (2010) model estimates a standard deviation of the order of one meter for all the reference velocities whether or not the reference velocity is close to the lock-in velocity. However, when the wind turbulence intensity dependency is incorporated, the tower tip standard deviation is much smaller than the previously estimated results, being of the order of centimeters. The differences between the remaining models is hardly appreciated due to the scale factor. Fig. 3(b) shows the same analysis, standard deviation as a function of reference velocity, for a turbulence intensity of 0.04. Due to the fact that Eurocode-1 (2010) model does not include the wind turbulence intensity dependency, the same results, standard deviations of the order of one meter, than Fig. 3(a) for Eurocode-1 (2010) model are obtained regardless of the reference velocity. Since the considered reference turbulence intensity is small, the model including the Reynolds number dependency and the wind turbulence intensity dependency presents similar results than Eurocode-1 (2010). On the other hand, Hansen (1998) model provides more reliable results from the point of view of consistency with experimental data, there is a velocity range, around the lock-in velocity, in which the structural dynamic response is larger.

On the other hand, the results presented in Fig. 3(a) and Fig. 3(b) evidence the importance of the turbulence levels quantified by the turbulence intensity in the dynamic response induced by vortex shedding. When the turbulence intensity is low enough,  $I_{\text{ref}} = 0.04$ , the maximum values for the standard deviation of the displacement at the tower top of the order of the tower top diameter. However, when the level of turbulence intensity is larger, the standard deviation of displacement at the tower top is lower. These results are in agreement with Eurocode-1 (2010) which mentions the influence of the turbulence intensity on the aerodynamic damping parameter although it does not propose any aerodynamic damping model which includes this dependency. It is observed that Eurocode-1 (2010) results are too conservatives compared to the other ones.

The previous analysis comparing the aerodynamic damping models evidences that in order to estimate the dynamic response and derived results as the fatigue damage, in light and low damped structures such as the case analyzed here for any external condition, it is necessary to model the dependencies of the aerodynamic damping parameter with the turbulence intensity and the reduced velocity in a proper way, for instance by means of the Hansen (1998) model.

#### 4. Fatigue analysis and results

As introduced in Section 1, and developed in Section 2, this paper addressed the fatigue assessment during the wind turbine tower erection defining the damage equivalent load. This section presents the fatigue assessment of the four geometric configurations shown in Fig. 1 whose modal properties are shown in Appendix A. These configurations correspond to the

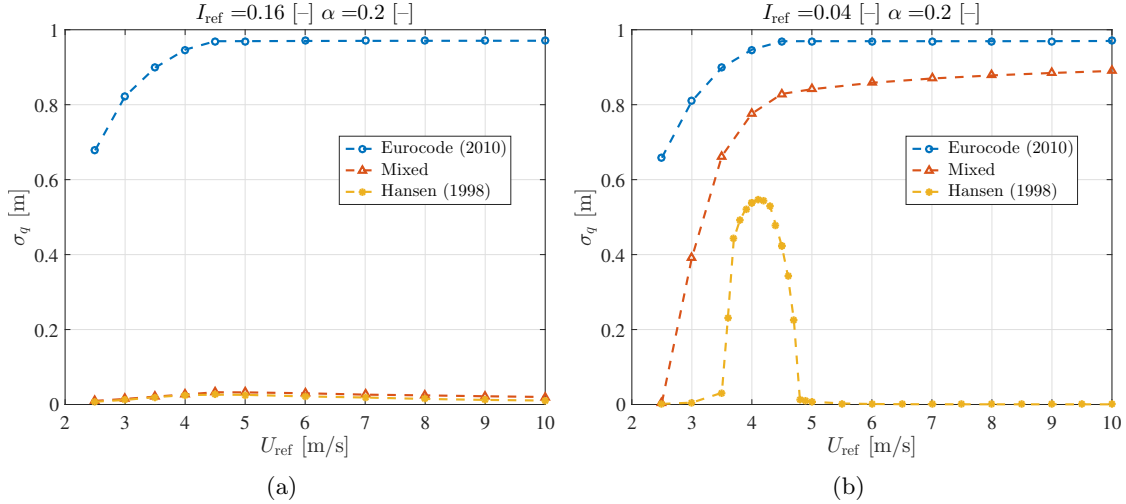


Fig. 3 Displacement standard deviation at the TG125-R tower tip as a function of the reference velocity,  $U_{\text{ref}}$ , for Eurocode-1 (2010) model,  $K_a(z) = K_{a_{\text{max}}}(\text{Re})$ , the mixed model,  $K_a(z) = K_{a_{\text{max}}}(\text{Re}) K_{I_u}(I_u)$ , and Hansen (1998) model,  $K_a(z) = K_{a_{\text{max}}}(\text{Re}) K_{I_u}(I_u) K_{U_r}(U_r)$ . In Fig. (a), the turbulence intensity is  $I_{\text{ref}} = 0.16$  and in Fig. (b)  $I_{\text{ref}} = 0.04$

tower configured by four sections (named as TG125-4); five sections (named as TG125-5); five-section tower with nacelle (named as TG125-G) and five-section tower with nacelle and stopped rotor (named as TG125-R). As regards the damage equivalent load computation, considering the analysis carried out in Section 3, the simulation time is fixed to  $t_{\text{sim}} = 3600$  s, the number of stochastic realizations averaged to  $N_{\alpha} = 24$  and the aerodynamic damping model of Hansen (1998) has been considered. On the other hand, the damage equivalent load is defined for 1000 cycles and the slope of the S-N fatigue curve is defined as  $m_f = 4$ . Due to the fact that the structural frequencies associated with the structural modes of each tower geometric configuration are sufficiently separated and the vortex shedding is a narrow-banded stochastic process, a sensitivity analysis has shown that two structural modes are enough to obtain the structural dynamic response. As for the vortex shedding phenomenon, considering the tower circular cross-section, the Strouhal number is set to 0.2.

Fig. 4 shows the damage equivalent load as a function of the reference velocity and of the reference turbulence intensity for the four geometric configurations considered, Fig. 4(a)-4(d) for TG125-R to TG125-4. The results have been calculated for a range of reference velocities of  $0 < U_{\text{ref}} < 20$  m/s. This figure is presented keeping the same ordinate axis scale. This choice enables to compare the four tower geometric configurations between them and between the reference turbulence intensity values. Although the ordinate axis scale prevents the maximum damage equivalent loads associated with the lower reference turbulence intensity values from being observed, their tendencies are quite similar between them. Fig. 5(a) presents the maximum damage equivalent load values. As regards the damage equivalent load tendency, for the four cases there is a velocity range in which the damage equivalent load is larger due to the fact that the vortices are shed with a frequency close to the first

resonance structural frequency. For those geometric configurations that are composed of a larger number of sections or present a point mass in its top, representing the nacelle and rotor, the largest value of damage equivalent load occurs at lower values of the reference velocity; since for these configurations the tower first resonance frequency is lower. As for the wind turbulent intensity analysis, two opposite actions occur depending on the reference intensity value. On the one hand, reducing the turbulence intensity causes the lift coefficient PSD bandwidth and the lift coefficient standard deviation to be reduced which provoke a narrower lock-in velocity range and a lower maximum damage equivalent load, see, for instance, Figs. 4(a) and 4(b) for  $I_{\text{ref}} = 0.16$  and  $I_{\text{ref}} = 0.12$ . On the other hand, reducing the turbulence intensity causes a more negative aerodynamic damping which leads to reduce the total damping, being the structure more sensitive to the vortex shedding loads and showing larger maximum damage equivalent load, see, for instance, Fig. 4(c) for  $I_{\text{ref}} = 0.16$  and  $I_{\text{ref}} = 0.12$ . Depending on the reference intensity value and the tower geometric configuration prevail one of the two commented actions. In addition, as has been mentioned above, when the lowest turbulence intensity values occur,  $I_{\text{ref}} = 0.08$  or  $I_{\text{ref}} = 0.04$ , depending on the tower geometric configuration, the damage equivalent load exceeds the maximum value of the ordinate axis and the largest damage equivalent loads take place. In these cases, the aerodynamic damping overcomes the structural one around the lock-in velocity which causes the structure to undergo large self-excitation and the largest fatigue damage.

The maximum values of the damage equivalent load are presented in Fig. 5(a) for each geometric configuration and for different values of turbulence intensity. This information enables to assess the severity of the fatigue damage depending on the geometric configuration and reflects the importance of the structural and geometric properties, such as the structural damping or the diameter distribution, which is linked to the aerodynamic damping parameter. Furthermore, it can be observed that the structural configuration is not the only variable that affects the magnitude of the damage equivalent load, being the turbulence intensity a driving parameter. The analysis reveals that higher turbulence intensity values,  $I_{\text{ref}} = 0.16$  or  $I_{\text{ref}} = 0.12$ , lead to the lowest fatigue damage equivalent loads. However, if the turbulence intensity is reduced,  $I_{\text{ref}} = 0.08$  or  $I_{\text{ref}} = 0.04$ , the maximum damage equivalent load is, depending on the tower geometric configuration, up to one order of magnitude higher than the previous values. For a fixed reference turbulence intensity value, considering fewer sections or tower configurations without nacelle and stopped rotor leads to larger damage equivalent loads as general rule. The reason is that the four-section and five-section towers present, in absolute value, a larger aerodynamic damping than the five-section tower with nacelle or with nacelle and stopped rotor. In order to explain the tendency change for the four-section tower, it is necessary to consider Eq. (15), cancelling the term related to the tower tip point mass. The remaining term is a sum of the product of two factors, which can be reduced to analyze the first structural mode. The first product factor is a constant value after doing the integral, and the second one is formed by the first mode coordinate, which is a function of time. Comparing the four-section tower with the five-section one, the TG125-4 constant value is, approximately, the double of the TG125-5 one. On the other hand, for any turbulence intensity value analyzed, the steady response value of the first mode coordinate associated with the TG125-4 is always smaller than the TG125-5, therefore, there are two

opposite actions working at the same time. When the reference turbulence intensity is set to  $I_{ref} = 0.08$ , the TG125-4 first mode coordinate is around five times smaller than the TG125-5 one which leads to a lower damage equivalent load of the TG125-4 structure. However, when the reference turbulence intensity is 0.04, the effect of the constant value overweighs the effect of the first mode coordinate contribution leading to a higher TG125-4 fatigue damage equivalent load.

The reference velocity which causes the maximum value of the fatigue damage equivalent load,  $U_{ref,DEL}$ , is shown in Fig. 5(b). From this information, it can be deduced that considering geometric configurations with less sections makes the maximum damage equivalent load take place at higher velocities. The reason has been mentioned previously and it is

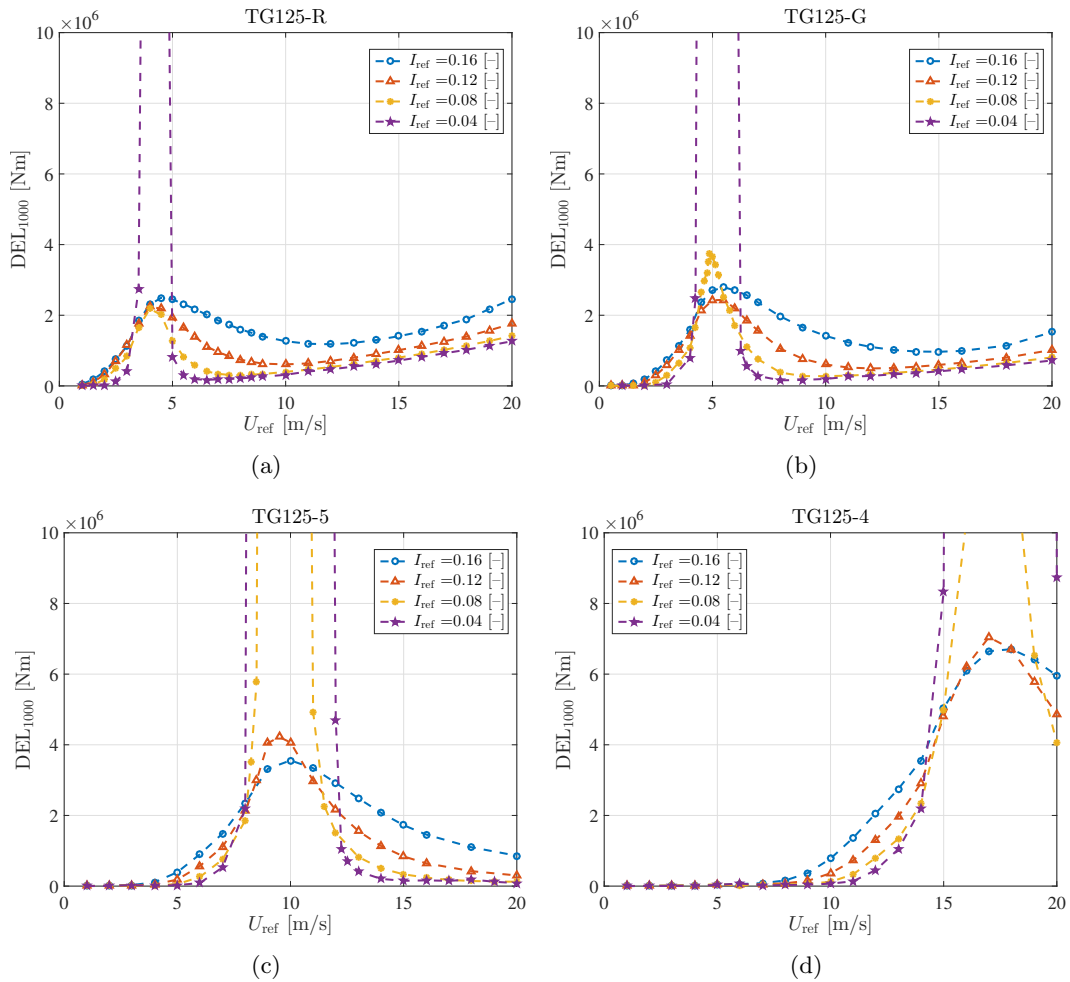


Fig. 4 Damage equivalent load, defined for  $N = 1000$  cycles,  $DEL_{1000}$ , as a function of the reference velocity and the turbulence intensity for TG125-R, TG125-G, TG125-5 and TG125-4 is shown in Figs. 4(a) - 4(d), respectively. The wind shear exponent is set to 0.2 and the slope of the S-N curve to 4

well known, these configurations have a higher first structural resonance frequency and, in consequence, also higher resonance velocities since the resonance occurs when the structural frequency is the same as the vortex shedding frequency which is related to the mean longitudinal velocity,  $f_{vs} = St U(z)/D(z)$ . On the other hand, the turbulence intensity has a little influence on such reference velocity values.

### 5. Discussion of assembly strategies

The analysis presented in Section 4 reveals that wind features (longitudinal mean velocity and turbulence intensity) and tower geometric configuration have a noticeable impact on the fatigue damage equivalent load experienced during assembly. Consequently, modeling these dependencies allows the definition of optimal assembly strategies oriented to minimize fatigue damage, enabling maintenance cost reduction in the long-term.

In order to define the mentioned assembly strategies which minimize the damage equivalent load, curves of damage equivalent load as a function of the reference velocity for several turbulence intensity values, from  $I_{ref} = 0.04$  to  $I_{ref} = 0.16$ , are obtained for the four tower geometric configurations shown in Fig. 1. As defined in Section 4, to compute the damage equivalent load, time series of 3600 s are obtained and a total of 24 stochastic realizations are averaged for each reference velocity. Equally to Section 4, the aerodynamic damping model of Hansen (1998) is used. Once the commented curves of damage equivalent load, equivalent to those obtained in Figs. 4(a)-4(d), are obtained for a velocity range of  $0 \text{ m/s} < U_{ref} < 60 \text{ m/s}$ , the minimum damage equivalent load for each reference velocity value is computed together with the tower geometric configuration which leads to this minimum condition. Figs. 6(a)-6(d) illustrate these results for each reference turbulence intensity value,  $I_{ref} = [0.16 \ 0.12 \ 0.08 \ 0.04]$ , respectively. Each figure is composed of two graphs, the upper one corresponds to the minimum damage equivalent load, while, the bottom one contains the information of the tower geometric configuration which minimizes the damage

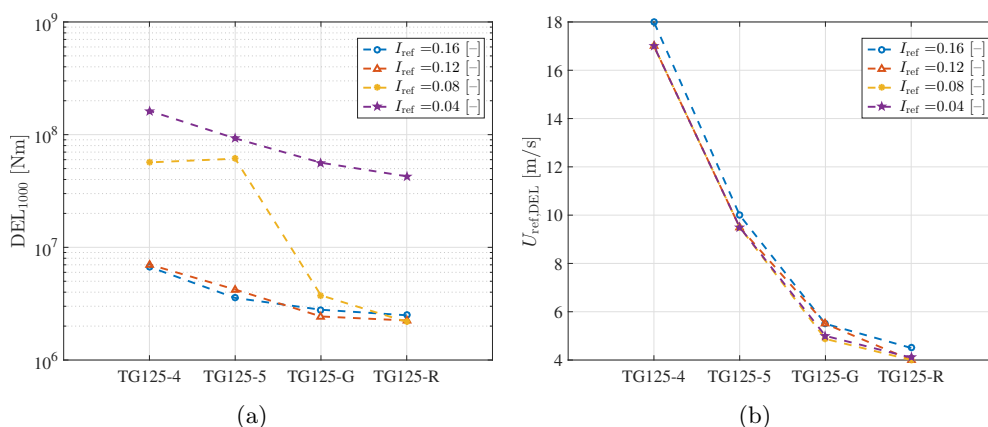


Fig. 5 Maximum value of the damage equivalent load,  $DEL_{1000}$ , Fig. (a), and the reference velocity,  $U_{ref,DEL}$ , which causes this maximum, Fig. (b), as a function of the geometric configuration

equivalent load.

As a general conclusion, regardless of the turbulence intensity, when the reference velocity is higher than, approximately, 30 m/s the four-section tower presents a lower fatigue damage equivalent load. Even when the velocity range is approximately from 20 m/s to 30 m/s the five-section tower shows the lower fatigue damage. Previous results indicates that lower wind turbine heights are less prone to suffer fatigue damage for the highest references velocities considered. For lower reference velocities, the best geometric configuration depends on the particular reference velocity and the turbulence intensity values. It should be noted that the tower composed of five section with nacelle and stopped rotor only produces minimum damage equivalent load for a narrower wind reference velocity range when the turbulence intensity is  $I_{\text{ref}} = 0.16$ , therefore, the TG125-R tower is not very appropriate from the fatigue damage point of view.

The potential use of the previous results is to select the geometric configuration during the assembly process using as input information a weather forecast, speeding up or delaying the assembly process as appropriate. For instance, if weather forecast predicts the arrival of a thunderstorm of wind velocity higher than 30 m/s, considering the previous results, the wind tower assembly process should stop erecting wind turbine tower stages, keeping the tower height at a minimum. However, if the weather forecast predicts a wind velocity of 20 m/s, the assembly should be speeded up to the TG125-5 tower configuration.

## 6. Conclusions

This paper presents a time domain approach to assess fatigue damage of wind turbine towers from the vortex shedding loads description stated by Vickery and Basu (1983b). From the fatigue damage assessment of tower geometric configurations during the wind turbine erection, an assembly strategy is proposed to minimize fatigue damage. Furthermore, the influence of three aerodynamics models has been analyzed which has demonstrated the necessity of considering Reynolds number, reduced velocity and turbulence intensity dependencies to obtain estimates with physical meaning when light and low damped structures are evaluated, such as the considered steel tower.

The fatigue damage assessment of several tower geometric configurations of a real wind turbine has revealed that low reference turbulence intensity values lead to self-excitement of the structure causing large damage equivalent loads. As regards the assembly strategy, it has been observed that lower tower wind turbine heights are less prone to suffer fatigue damage in the presence of higher reference velocity values typical of thunderstorms. In addition, it has been observed that the most disadvantaged tower geometric configuration for minimizing the damage equivalent load is the one composed of five section, nacelle and stopped rotor.

New experimental tests to obtain a better description of the aerodynamic damping parameter with turbulence intensity and velocity are required in order to improve the existing dynamic models. In addition, future works should address how to include the aerodynamic effect of nacelle and rotor, since their aerodynamic effects have been neglected.

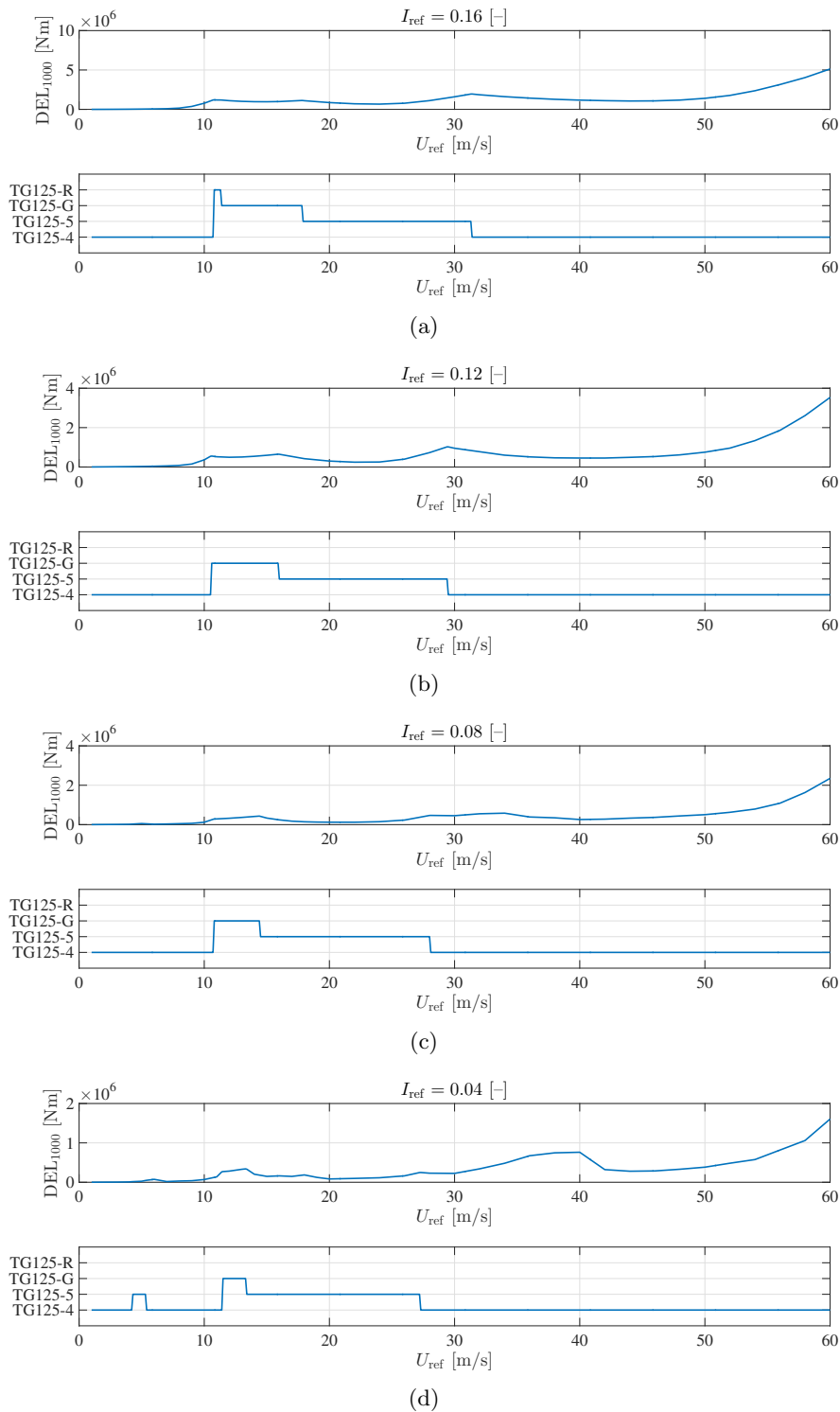


Fig. 6 Minimum fatigue damage equivalent load among all tower configurations, see Fig. 1, as a function of the reference velocity, for the four turbulence intensity conditions considered, Figs. (a)-(d). For each subfigure, upper graph shows the minimum damage equivalent load while bottom graph presents the tower geometric configuration leading to those minimum values. The wind shear exponent is set to 0.2

### Acknowledgments

This research has been funded by the CATEDRA GAMESA of the Universidad Politecnica de Madrid as a part of the research grant “Loads estimation on wind turbine towers during the assembly process due to vortex shedding”. This support is gratefully acknowledged. The authors also would like to thank Mr. Yago Urroz Castillo, wind turbine loads and dynamics engineer of GAMESA, for providing data and simulated aeroelastic results of the analyzed wind turbine tower which have played an important role in the model verification and validation.

### Appendix A. Tower data

This appendix provides the modal structural information and geometric information related to the tower geometric configurations considered in Section 3 and 4. Table 1 shows the modal information: structural frequencies, modal masses and structural damping coefficients, for the first two structural modes while Figs. 7(a) and 7(b) provide the first and second structural modes for the four geometric configurations considered. Fig. 8 presents the tower diameter distribution needed to compute the vortex shedding forces and the aerodynamic damping. The four-section tower maximum height is 90.62 m.

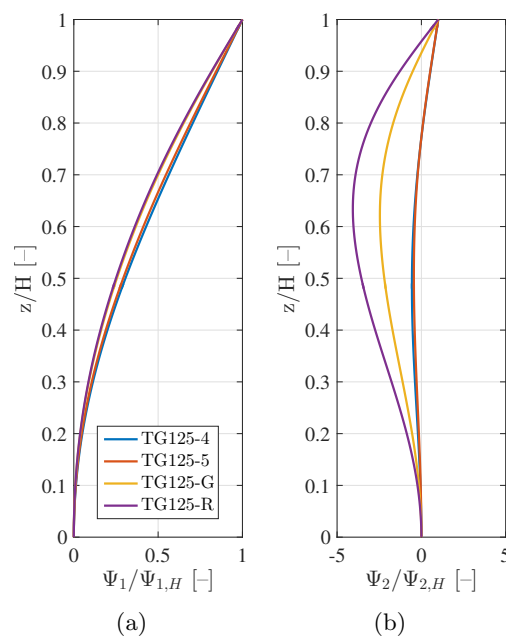


Fig. 7 Two first modes of the four geometric configurations considered expressed in nondimensional form with the displacement reached at the tower tip and as a function of the nondimensional height. In (a) the first mode is presented and in (b) the second one

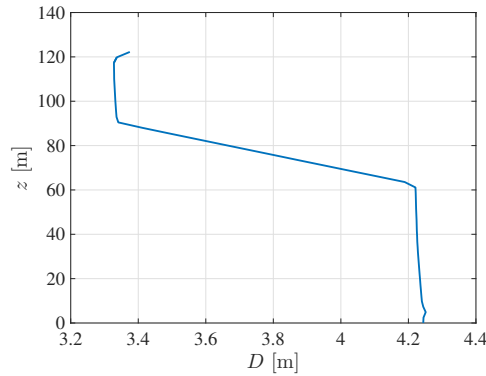


Fig. 8 Diameter distribution of the five-section tower. When the four-section tower, TG125-4, is considered the diameter distribution ends at 90.62 m

Table 1 Modal information about the first two modes of the analyzed tower composed of four sections, five sections, five sections with nacelle and five sections with nacelle and stopped rotor, see Fig. 1.  $f_{s,j}$  are the structural frequencies,  $m_j$  the modal masses and  $c_j$  the aerodynamic damping coefficients

		TG125-4	TG125-5	TG125-G	TG125-R
$f_{s,j}$ (Hz)	First	0.7174	0.4389	0.2295	0.1821
	Second	3.6298	1.9480	1.3833	1.3369
$m_j$ (kg)	First	$4.1246 \times 10^4$	$3.8358 \times 10^4$	$3.4066 \times 10^4$	$3.3484 \times 10^4$
	Second	$3.6648 \times 10^4$	$2.8849 \times 10^4$	$5.8537 \times 10^5$	$1.5902 \times 10^6$
$c_j$ (kg/s)	First	$1.8592 \times 10^3$	$1.0578 \times 10^3$	$4.9123 \times 10^2$	$3.8319 \times 10^2$
	Second	$1.3373 \times 10^4$	$5.6498 \times 10^3$	$8.1403 \times 10^4$	$2.1372 \times 10^5$

**References**

ASTM (1985), *Standard Practices for Cycle Counting in Fatigue Analysis*, Technical Report ASTM Standard E1049-85, ASTM International.

Belver, A.V., Iban, A.L. and Martin, C.E.L. (2012), “Coupling between structural and fluid dynamic problems applied to vortex shedding in a 90 m steel chimney”, *J. Wind Eng. Industr. Aerodyn.*, **100**(1), 30-37.

Berny-Brandt, E.A. and Ruiz, S.E. (2016), “Reliability over time of wind turbines steel towers subjected to fatigue”, *Wind Struct.*, **3**(1), 75-90.

Chen, X. (2013), “Estimation of stochastic crosswind response of wind-excited tall buildings with nonlinear aerodynamic damping”, *Eng. Struct.*, **56**, 766-778.

Chen, X. (2014), “Analysis of crosswind fatigue of wind-excited structures with nonlinear aerodynamic damping”, *Eng. Struct.*, **74**, 145-156.

Dyrbye, C. and Hansen, S. (1997), *Wind Loads on Structures*, Wiley.

E1049-85, A.S. (1985), *Standard Practices for Cycle Counting in Fatigue Analysis*, Annual Book of ASTM Standars, ASTM International, **3**.

Eurocode-1 (2010), *Actions on Structures. Part 1-4: General Actions- Wind Actions*, Technical Report BS EN 1991-1-4:2005+A1:2010, British Standards.

- Gorski, P. (2009), "Some aspects of the dynamic cross-wind response of tall industrial chimney", *Wind Struct.*, **12**(3), 259-279.
- Hansen, S. (1998), "Vortex-Induced vibrations of line-like structures", *CICIND Rep.*, **15**(4), 15-23.
- IEC-61400-1 (2003), *Part 1: Safety Requirements*, Wind Turbine Generator Systems IEC 61400-1, Edition 3, International Electrotechnical Commission.
- Llorente Gonzalez, J.I. (2006), *Tool for Preventing the Vortex Effect*, WO Patent App. PCT/ES2006/000,148.
- Nguyen, T.C., Huynh, T.C. and Kim, J.T. (2015), "Numerical evaluation for vibration-based damage detection in wind turbine tower structure", *Wind Struct.*, **21**(6), 657-675.
- Nguyen, T.C., Huynh, T.C., Yi, J.H. and Kim, J.T. (2017), "Hybrid bolt-loosening detection in wind turbine tower structures by vibration and impedance responses", *Wind Struct.*, **24**(4), 385-403.
- Niesłony, A. (2009), "Determination of fragments of multiaxial service loading strongly influencing the fatigue of machine components", *Mech. Syst. Sign. Proc.*, **23**(8), 2712-2721.
- Ragan, P. and Manuel, L. (2007), "Comparing estimates of wind turbine fatigue loads using time-domain and spectral methods", *Wind Eng.*, **31**(2), 83-99.
- Repetto, M.P. and Solari, G. (2002), "Dynamic crosswind fatigue of slender vertical structures", *Wind Struct.*, **5**(6), 527-542.
- Repetto, M.P. and Solari, G. (2010), "Wind-induced fatigue collapse of real slender structures", *Eng. Struct.*, **32**(12), 3888-3898.
- Ruscheweyh, H. (1994), *Vortex Excited Vibrations*, in *Wind-Excited Vibrations of Structures*, Springer, 51-84.
- Shinozuka, M. and Deodatis, G. (1991), "Simulation of stochastic processes by spectral representation", *Appl. Mech. Rev.*, **44**(4), 191-204.
- Tranvik, P. and Alpsten, G. (2002), *Dynamic Behaviour under Wind Loading of a 90 m Steel Chimney*, Report 9647-3, Alstom Power Station AB.
- Trivellato, F. and Castelli, M.R. (2015), "Appraisal of Strouhal number in wind turbine engineering", *Renew. Sustain. Energy Rev.*, **49**, 795-804.
- Veers, P.S. (1988), *Three-Dimensional Wind Simulation*, Technical Report SAND-88-0152C, Sandia National Labs., Albuquerque, NM, U.S.A.
- Verboom, G. and Van Koten, H. (2010), "Vortex excitation: Three design rules tested on 13 industrial chimneys", *J. Wind Eng. Industr. Aerodyn.*, **98**(3), 145-154.
- Vickery, B. and Basu, R. (1983a), "Across-wind vibrations of structure of circular cross-section. Part II. Development of a mathematical model for full-scale application", *J. Wind Eng. Industr. Aerodyn.*, **12**(1), 75-97.
- Vickery, B. and Basu, R. (1983b), "Across-wind vibrations of structures of circular cross-section. Part I. Development of a mathematical model for two-dimensional conditions", *J. Wind Eng. Industr. Aerodyn.*, **12**(1), 49-73.
- Vickery, B. and Basu, R. (1984), "The response of reinforced concrete chimneys to vortex shedding", *Eng. Struct.*, **6**(4), 324-333.
- Vickery, B.J. and Clark, A.W. (1972), "Lift or across-wind response to tapered stacks", *J. Struct. Div.*, **98**(1), 1-20.